Neuromuscular Stochastic Optimal Control of a Tendon Driven Index Finger Model

Evangelos Theodorou, Emanuel Todorov and Francisco J. Valero-Cuevas

Abstract— Our long-term goal is to find control princi-
ples to control robotic hands with dexterity and robustness
comparable to that of the human hand. Here we explore a
control strategy capable of accommodating the nonlinearities,
high dimensionality and endogenous noise intrinsic to complex,
tendon-driven biomechanical structures. We present the first
stochastic optimal feedback controller (i.e., an iterative Linear
Quadratic Gaussian controller) applied to a tendon-driven
simulated robotic index finger model. In our model we take
into account both the tendon network driving of the index
finger, and we consider first-order muscle activation-contraction
dynamics. Our feedback controller shows robustness against
noise and perturbation of the dynamics. Moreover, it can
also successfully overcome the nonlinearities intrinsic to the
mechanics of the finger for large postural changes, and the
need for non-negative control signals. Our simulations provide,
for the first time, the complete time history of tendon tensions,
lengths and velocities for the tasks of tapping with nonzero
terminal velocities required for dynamic manipulation.

We find that the optimal control of realistic tendon-driven
systems fundamentally stretches current methods to their limits.
To find a successful control strategy, the algorithm and user
must overcome several critical challenges inherent to the control
of tendon-driven fingers systems in which all uni-directional
control commands can actuate all joints (either directly or
through dynamic coupling). Therefore, all elements of the so-
lution are interwoven including the tuning of the cost function,
the dynamics of the plant, and the initial guesses for state and
control trajectories.

I. INTRODUCTION

Despite the work to build "smart" biologically inspired
robotic hands, there is no mechanical hand that can compete
the robustness and the dexterity of the hand in tasks such
as grasping objects with uncertain loads and various shapes,
playing music instruments, or manipulating objects.

The gap in the functionality and robustness between
robotic and human hands has its origins in our lack of
understanding of design principles based on solid control
theoretic principles applicable to complex bio-mechanical
structures such as the hand.

From the control theoretic standpoint, the control of a
highly dimensional and nonlinear stochastic plant of the
complexity of a robotic or biomechanical hand is not an easy
task–which also makes it difficult to understand the neuro-
muscular control of the handmanipulation. To appreciate the
high dimensionality, it is enough to consider that more than
35 tendons must be controlled by the nervous system. Some
critical questions that remain open are:

- What strategies does the nervous system use for moving
  the finger given the geometrical and mechanical char-
  acteristics of the muscular-tendon-bone structure? What
  are the underlying tensions applied to tendons? What is
  the role of each tendon?

Our recent experimental work [5] investigated the neu-
ral control of contact transition between motion and force
during tapping. In [4] we found that such transitions from
motion to well-directed contact force are a fundamental part
of dexterous manipulation, and that such tasks are likely
controlled optimally. Moreover, one of the main assumption
in [4] is that the underlying control strategy of the finger is
considered to be open loop. In addition, the neuromuscular
delays are modeled as activation contraction dynamics at the
level of the torques driving the 3 joints of the index finger.
Even though with this simple model the optimality principles
of the motion to force transition for the task of tapping
were investigated, an open loop control strategy would have
failed in tasks such as object manipulation where feedback
control is critical requirement for successfully performing
the manipulation task. Furthermore, since only 3 sets of
differential equation that model the activation contraction
dynamics are considered, the full structure and redundancy
of the index finger is was not explored.

Motivated by the limitations of previous work, we address
the problem of controlling the index finger in the framework
of stochastic optimal feedback control theory. In particular,
we make use of the iterative Linear Quadratic Gaussian
controller (iLQG) - one of the few methods in optimal
control that can handle nonlinear dynamical systems with
complexity and dimensionality equivalent to the complexity
and dimensionality of the index finger. Our index finger
model is based on the accurate biomechanical model in [1]
driven by 11 tendons. Our stochastic optimal controller gives
us the complete time history of the tendon lengths and tendon
velocities for the tasks of tapping with nonzero, as well as
the resulting 11 tensions applied from the tendons to the
bone structure of the index finger, and torques at the 3 joints
of the index finger. The information regarding the tension
profiles of the tendons is of critical importance to the field
of neuromuscular control of the hand since because it sheds
light into the underlying patterns of force production at the
level of individual muscles. Furthermore it also illustrates
the synergetic mechanism as a requirement for the central
nervous system to control the index finger.

This paper is organized as follows: in section II we discuss
the index finger model. In section II-A we derive the moment
arm matrix of the index finger. In section IV we discuss the
iLQG framework and provide the main equations while in
II-B we provide the overall dynamic system which includes
the multibody dynamics. We then show our simulation results

for the tapping task with index finger under non-zero and we analyze the results regarding the underlying kinetics of the tendon structure of the index finger. Finally in the last section we present our conclusions and discuss future work.

II. INDEX FINGER MODEL

The skeleton of the human index finger consist of 3 joints connected with 3 rigid links. The two joints (proximal interphalangeal (PIP) and the distal interphalangeal (DIP)) are described as hinge joints that can generate both flexion-extension. The metacarpophalangeal joint (MCP) is a saddle joint and it can generated flexion-extension as well as abduction-adduction. Fingers have at least 6 muscles, and the index finger is controlled by 7. Starting with the flexors, the index finger has the Flexor Digitorum Profundus (FDS) and the Flexor Digitorum Superficialis (FDP). The the Radial Interosseous (RI) acts on the MCP joint. Lastly, the extensor mechanism acts on all three joints. It is an interconnected network of tendons driven by two extensors Extensor Communis (EC) and the Extensor Indicis (EI), and the Ulnar Interosseous (UI) and Lumbrical (LU). We also include 4 passive tendon elements that complete this network. These passive tendons are the Terminal Extensor (TE), the Radial Band (RB) the Ulnar Band (UB) and the Extensor Slip (ES). We simulate 11 tendons in total, 7 active (i.e., driven by independently controlled muscles) and 4 passive. The basic equation for modeling the tendon lengths L according to [1] is given by:

$$L = \theta d + 2y \left(1 - \frac{\theta/2}{\tan(\theta/2)} \right) \quad (1)$$

where d is the distance from the straight part of the tendon towards the long axis and θ is the corresponding angle rotation. The term y corresponds to the distance from the end of the straight part towards the joint centre (i.e., moment arm). This distance is measure along the axis of the bone. A second order polynomial approximation of the equation above is formulated as $L = (b + h\theta)\theta$, where b and h are constants. With the exception of FDS and FDP, the equation above is used for modeling the lengths of tendons that are involved in flexion-extension as well as for abduction - adduction. A subscript, a, will be used to denote the dependence of the tendon length of the abduction-adduction motion, with ϕ being the adduction angle.

For the FDS and FDP tendons we decided to use the more accurate model for tendon length (1) since these tendons depend on the majority of rotational variables. More precisely,the length of FDS depends on $\theta_1, \theta_2, \theta_3$ and ϕ while the length of FDP depends on θ_1, θ_2 and ϕ. Obviously, the use of approximated model $L = (b + h\theta)\theta$ for the case of FDS and FDP would have caused higher approximation errors than for the case of tendons which depend only on 1 or 2 rotational variables. More precisely we will have

$$
\begin{aligned}
L^{FDP} = {} & \theta_1 d_1^{FDP} + 2y_1^{FDP} \left(1 - \frac{\theta_1/2}{\tan(\theta_1/2)} \right) \\
+ {} & \theta_2 d_1^{FDP} + 2y_2^{FDP} \left(1 - \frac{\theta_2/2}{\tan(\theta_2/2)} \right) \\
+ {} & \theta_3 d_3^{FDP} + 2y_3^{FDP} \left(1 - \frac{\theta_3/2}{\tan(\theta_3/2)} \right) \\
+ {} & \left(b_a^{FDP} + h_a^{FDP}\phi \right) \phi \quad (2)
\end{aligned}
$$

$$
\begin{aligned}
L^{FDS} = {} & \theta_1 d_1^{FDS} + 2y_1^{FDS} \left(1 - \frac{\theta_1/2}{\tan(\theta_1/2)} \right) \\
+ {} & \theta_2 d_1^{FDS} + 2y_2^{FDS} \left(1 - \frac{\theta_2/2}{\tan(\theta_2/2)} \right) \\
+ {} & \left(b_a^{FDS} + h_a^{FDS}\phi \right) \phi \quad (3)
\end{aligned}
$$

The tendon length mechanism for EC and TE is rather simple due to their dependence on the rotation of only one joint. The tendon extensor for EC is a function of the rotation at the DIP join while the tendon length of TE is function of the rotation at the PIP joint.

$$L^{TE} = -r^{TE}\theta_3, \qquad L^{ES} = -r^{ES}\theta_2 \quad (4)$$

The tendon lengths of the RB and UB are functions of the rotation around the PIP joint with the addition of the terminal extensor.

$$L^{RB} = - \left(b^{RB} + h_{RB}\theta_2 \right) \theta_2 + \beta^{RB} E^{TE} \quad (5)$$

$$L^{UB} = - \left(b^{UB} + h_{UB}\theta_2 \right) \theta_2 + \beta^{UB} E^{TE} \quad (6)$$

For the RI the tendon length is a function of the MCP rotation only that includes flexion - extension and abduction - adduction. Therefore the tendon length is formulated as follows:

$$
\begin{aligned}
L^{RI} = {} & \left(b^{RI} + h_{RI}\theta_1 \right) \theta_1 \\
- {} & \left(b_a^{RI} + h_a^{RI}\phi \right) \phi \quad (7)
\end{aligned}
$$

Similarly, the tendon length for the LI is a function of the MCP rotation but with the addition of the tendon length of the UB. Consequently the LI tendon length is formulated by the following equation:

$$
\begin{aligned}
L^{LI} = {} & \left(b^{UI} + h_{UI}\theta_1 \right) \theta_1 \\
- {} & \left(b_a^{UI} + h_a^{UI}\phi \right) \phi + L^{UB} \quad (8)
\end{aligned}
$$

The length of the LU tendon is a function of the MCP rotation with the addition of the UB and the subtraction of the FDP tendon lengths . The length of FDP is subtracted from the total lengths of LU since the origin of LU is on FDP. Thus we will have that:

$$
\begin{aligned}
L^{LU} &= \left(b^{LU}+h_{LU}\theta_1\right)\theta_1 \\
&\quad - \left(b_a^{LU}+h_a^{LU}\phi\right)\phi \\
&\quad + L^{RB}-L^{FDP}
\end{aligned} \tag{9}
$$

Finally the tendon lengths of the main extensors of the index finger, EC and EI are function of the MCP rotation and with the addition of the displacements that are transformed to the next joints PIP and DIP through the extensor mechanism.

$$
\begin{aligned}
L^{EC} &= -r^{EC}\theta_1 - \left(b_a^{EC}+h_a^{EC}\theta_1\right)\theta_1 \\
&\quad + \min\left(L_1,L_2,L_3\right)
\end{aligned} \tag{10}
$$

and

$$
\begin{aligned}
L^{EI} &= -r^{EI}\theta_1 - \left(b_a^{EI}+h_a^{EI}\phi\right)\phi \\
&\quad + \min\left(L_1,L_2,L_3\right)
\end{aligned} \tag{11}
$$

where the terms L_1,L_2 and L_3 are defined as follows:

$$
\begin{aligned}
L_1 &= L^{ES} \tag{12} \\
L_2 &= L_{UB}+\left(1-\beta^{UB}\right)L^{TE} \tag{13} \\
L_3 &= L_{RB}+\left(1-\beta^{RB}\right)L^{TE} \tag{14}
\end{aligned}
$$

In this work we have slightly modified the extensor mechanics for the EI and the EC tendons to avoid the nonlinear operator min by assuming that:

$$
\begin{aligned}
L^{EC} &= -r^{EC}\theta_1 - \left(b_a^{EC}+h_a^{EC}\theta_1\right)\theta_1 \\
&\quad + E\left(L_1,L_2,L_3\right)
\end{aligned} \tag{15}
$$

$$
\begin{aligned}
L^{EI} &= -r^{EI}\theta_1 - \left(b_a^{EI}+h_a^{EI}\phi\right)\phi \\
&\quad + E\left(L_1,L_2,L_3\right)
\end{aligned} \tag{16}
$$

with the length function $E\left(L_1,L_2,L_3\right)$ defined as $E\left(L_1,L_2,L_3\right)=\sum_{j=1}^{3}w_jL_j$ with $\sum_{j=1}^{3}w_j=1$ and $w_j>0\forall j=1,2,3$. There are 39 parameters for the equations 11 tendons lengths of the index which are provided in table I.

A. Index Finger Moment Arm

Since the tendon lengths have been defined for the 11 tendons of the index finger, the moment arm matrix for the 7 active tendons can been found according to the equation:

$$
\mathbf{M}\left(\Theta\right)=\nabla_{\Theta}\mathbf{L} \tag{17}
$$

where $\Theta=\left(\theta_1,\theta_2,\theta_3,\phi\right)^T$ and $\mathbf{L}\in\Re^{7\times1}$ defined as $\mathbf{L}=\left(L^{FDS},L^{FDP},L^{LU},L^{RI},L^{LU},L^{EC},L^{EI}\right)^T$. More precisely the moment arm vector for the FDP tendons is expressed as $\mathbf{M}_{\Theta}^{FDP}=\left(M_{\theta_1}^{FDP},M_{\theta_2}^{FDP},M_{\theta_3}^{FDP},M_{\phi}^{FDP}\right)$ where $\forall i=1,2,3$ we have that

$$
M_{\theta_i}^{FDP}=d_i^{FDP}+y_i^{FDP}\left(\frac{\sin\left(\theta_i\right)-\theta_i}{2\sin^2\left(\theta_i\right)}\right) \tag{18}
$$

and $M_{\phi}^{FDP}=h_a\phi$. In cases where $\theta_i=0$ then the moment arm of the FDP is given by the following equation $\lim_{\theta_i\to0}M_{\theta_i}^{FDP}=d_i^{FDP}$, $\forall i=1,2,3$. The moment arm vector for the FDS tendon is expressed as $\mathbf{M}_{\Theta}^{FDS}=\left(M_{\theta_1}^{FDS},M_{\theta_2}^{FDS},M_{\theta_3}^{FDS},M_{\phi}^{FDS}\right)$ where $\forall i=1,2$ we have that:

$$
M_{\theta_i}^{FDS}=d_i^{FDS}+y_i^{FDS}\left(\frac{\sin\left(\theta_i\right)-\theta_i}{2\sin^2\left(\theta_i\right)}\right) \tag{19}
$$

$$
\tag{20}
$$

and $M_{\theta_3}^{FDS}=0$, $M_{\phi}^{FDS}=h_a\phi$. Similarly when $\theta_i=0$ then the moment arm of the FDS is given by the following equation:$\lim_{\theta_i\to0}M_{\theta_i}^{FDS}=d_i^{FDS}\forall i=1,2$. For the LU tendon the moment arm vector is expressed as:

$$
\mathbf{M}_{\Theta}^{LU}=\begin{bmatrix}M_{\theta_1}^{LU}\\M_{\theta_2}^{LU}\\M_{\theta_3}^{LU}\\M_{\phi}^{LU}\end{bmatrix}=\begin{bmatrix}b^{LU}+h^{LU}\theta_1-M_{\theta_1}^{FDP}\\M_{\theta_2}^{RB}-M_{\theta_2}^{FDP}\\M_{\theta_3}^{RB}-M_{\theta_3}^{FDP}\\-b_a^{LU}-h_a^{LU}\phi-M_{\phi}^{FDP}\end{bmatrix} \tag{21}
$$

Similarly for the UI and RI tendons we will have

$$
\mathbf{M}_{\Theta}^{RI}=\begin{bmatrix}M_{\theta_1}^{RI}\\M_{\theta_2}^{RI}\\M_{\theta_3}^{RI}\\M_{\phi}^{RI}\end{bmatrix}=\begin{bmatrix}b^{RI}+h^{RI}\theta_1\\0\\0\\b_a^{RI}+h_a^{RI}\phi\end{bmatrix} \tag{22}
$$

and

$$
\mathbf{M}_{\Theta}^{UI}=\begin{bmatrix}M_{\theta_1}^{UI}\\M_{\theta_2}^{UI}\\M_{\theta_3}^{UI}\\M_{\phi}^{UI}\end{bmatrix}=\begin{bmatrix}b^{UI}+h^{UI}\theta_1\\M_{\theta_2}^{UB}\\M_{\theta_3}^{UB}\\b_a^{UI}+h_a^{UI}\phi\end{bmatrix} \tag{23}
$$

As we can see from above the moment arm vectors for UI and RI are function of the moment arm vectors of UB and RB tendons which are defined as follows

$$
\mathbf{M}_{\Theta}^{UB}=\begin{bmatrix}M_{\theta_1}^{UB}\\M_{\theta_2}^{UB}\\M_{\theta_3}^{UB}\\M_{\phi}^{UB}\end{bmatrix}=\begin{bmatrix}0\\-(b^{UB}+h^{UB}\theta_2)\\-r^{TE}\\0\end{bmatrix} \tag{24}
$$

and

$$
\mathbf{M}_{\Theta}^{RB}=\begin{bmatrix}M_{\theta_1}^{RB}\\M_{\theta_2}^{RB}\\M_{\theta_3}^{RB}\\M_{\phi}^{RB}\end{bmatrix}=\begin{bmatrix}0\\-(b^{RB}+h^{RB}\theta_2)\\-r^{TE}\\0\end{bmatrix} \tag{25}
$$

Finally, the moment arm vectors of the main extensor tendons EC and EI of the index finger are expresses as:

$$
\mathbf{M}_{\Theta}^{EC}=\begin{bmatrix}M_{\theta_1}^{EC}&M_{\theta_2}^{EC}&M_{\theta_3}^{EC}&M_{\phi}^{EC}\end{bmatrix}^T= \tag{26}
$$

$$
=\begin{bmatrix}-r^{EC}\\-w_1r^{ES}-w_2(b^{UB}+h^{UB}\theta_2)-w_3(b^{RB}+h^{RB}\theta_2)\\-w_2r^{TE}-w_3r^{TE}\\-b_a^{EC}+h_a^{EC}\phi\end{bmatrix} \tag{27}
$$

Tendon(Joint)	r	b	h	d	y	ba	ha
TE(DIP)	1.88	-	-	-	-	-	-
FDP(DIP)	-	-	2.97	3.96	-	-	-
ES(PIP)	2.92	-	-	-	-	-	-
RB	-	2.54	-0.47	-	-	-	-
UB	-	1.7	0.57	-	-	-	-
FDS	-	-	-	4.13	6.73	-	-
FDP	-	-	-	5.76	7.5	-	-
EC(MCP)	8.3	-	-	-	-	2.08	-0.09
EI	8.82	-	-	-	-	0.59	0.8
RI	-	5.62	-1.29	-	-	5.63	0.54
UI	-	18.76	-8.16	-	-	5.77	0.03
LU	-	12.53	-2.17	-	-	4.96	-0.18
FDS	-	-	-	9.56	8.14	1.1	0.68
FDP	-	-	-	8.32	8.32	0.52	0.66

TABLE I

PARAMETERS FOR THE TENDON LENGTHS OF THE INDEX FINGER
MODEL.

Joint	Tendons
DIP	Terminal Extensor (TE)
	Flexor Digitorum Profundus (FDP)
PIP	Extensor Slip (ES)
	Radial Band (RB)
	Ulnar Band (UB)
	Flexor digitorum superficialis (FDS)
	Flexor digitorum profundus (FDP)
MCP	Extensor digitorum Communis (EC)
	Extensor indicis (EI)
	Radial Interosseous (RI)
	Ulnar Interosseous (UI)
	Lumbrical (LU)
	Flexor digitorum superficialis (FDS)
	Flexor digitorum profundus (FDP)

TABLE II

CORRESPONDENCE OF THE 7 ACTIVE TENDONS OF THE INDEX FINGER
WITH THE 3 JOINTS MCP, PIP AND DIP.

and

$$\mathbf{M}_{\Theta}^{EI} = \begin{bmatrix} M_{\theta_1}^{EI} & M_{\theta_2}^{EI} & M_{\theta_3}^{EI} & M_{\phi}^{EI} \end{bmatrix}^T =$$
$$= \begin{bmatrix} -r^{EI} \\ -w_1 r^{ES} - w_2(b^{UB} + h^{UB}\theta_2) - w_3(b^{RB} + h^{RB}\theta_2) \\ -w_2 r^{TE} - w_3 r^{TE} \\ -b_a^{EI} + h_a^{EI}\phi \end{bmatrix}$$
(28)

The moment arm matrix for the active tendons $\mathbf{M}_{\Theta}$ is therefore defined:

$$\begin{bmatrix} \mathbf{M}_{\Theta}^{FDP} & \mathbf{M}_{\Theta}^{FDP} & \mathbf{M}_{\Theta}^{LU} & \mathbf{M}_{\Theta}^{UI} & \mathbf{M}_{\Theta}^{RI} & \mathbf{M}_{\Theta}^{EI} & \mathbf{M}_{\Theta}^{EC} \end{bmatrix}$$ (29)

Since the tendon length is a function $\Theta(t)$ the velocity with which the tendon length changes over time is given by $\frac{dL(\Theta)}{dt} = \frac{\partial L(\Theta)}{\partial \Theta} \frac{\partial \Theta}{\partial t}$. Thus we will have that: $\mathbf{V}(\Theta, \dot{\Theta}) = \mathbf{M}_{\Theta} \times \dot{\Theta}$ where $\mathbf{M}_{\Theta} = \frac{\partial L(\Theta)}{\partial \Theta}$ and $\dot{\Theta} = \frac{\partial \Theta}{\partial t}$.

B. Index Finger Dynamics

The full model of the index finger is given by the equations that follow:

$$\ddot{\theta} = -\mathbf{I}(\theta)^{-1} \cdot \mathbf{C}(\theta, \dot{\theta}) + \mathbf{I}(\theta)^{-1} \cdot \mathbf{T}$$ (30)
$$\mathbf{T} = \mathbf{M}(\theta) \cdot \mathbf{F}$$ (31)
$$\dot{\mathbf{F}} = -\frac{1}{\tau}(\mathbf{F} - \mathbf{u})$$ (32)
$$\mathbf{u} > 0$$ (33)

where $\mathbf{I} \in \Re^{6 \times 6}$ is the inertial matrix and $\mathbf{C}(\theta, \dot{\theta}) \in \Re_{6 \times 1}$ is matrix of Coriolis and centripetal forces. The matrix $\mathbf{M} \in \Re^{3 \times 7}$ is the moment-arm matrix, $\mathbf{T} \in \Re^{3 \times 1}$ is the torque vector, $\mathbf{F} \in \Re^{7 \times 1}$ is the force-tension on the tendons and $\mathbf{u}$ is the control vector. Equation (32) is used to model delays in the generation of tensions on the tendons. For our simulations we have excluded the abduction-adduction movement at MCP joint and we examine planar movements and we investigate the necessary length and velocity profiles of the tendons for producing such movements. Therefore, the state space formulation of our model has dimensionality of 13, corresponding to 6 states related to joint space kinematics (angles and velocities) and 7 states for the tensions applied on the 7 active tendons. The quantities θ and $\dot{\theta}$ are vectors of dimensionality $\theta \in \Re^{3 \times 1}, \dot{\theta} \in \Re^{3 \times 1}$ defined as $\theta = (\theta_1, \theta_2, \theta_3)$ and $\dot{\theta} = (\dot{\theta}_1, \dot{\theta}_2, \dot{\theta}_3)$. The inertia $\mathbf{I}(\theta)$ terms of the forward dynamics are given as follows:

$$I_{11} = I_{31} + \mu_1 + \mu_2 + 2\mu_4 \cos \theta_2$$
$$I_{21} = I_{22} + \mu_4 \cos \theta_2 + \mu_6 \cos(\theta_2 + \theta_2)$$
$$I_{22} = I_{33} + \mu_2 + 2\mu_5 \cos \theta_3$$
$$I_{31} = I_{32} + \mu_6 \cos(\theta_3 + \theta_3)$$
$$I_{33} = \mu_3$$

while the term of coriolis and centripetal forces $\mathbf{C}(\theta, \dot{\theta})$ is formulated as follows:

$$C_1 = \mu_4 \sin \theta_2 \left[-\dot{\theta}_2 \left(2\dot{\theta}_1 + \dot{\theta}_2 \right) \right]$$
$$+ \mu_5 \sin \theta_3 \left[-\dot{\theta}_3 \left(2\dot{\theta}_1 + 2\dot{\theta}_2 + \dot{\theta}_3 \right) \right]$$
$$- \mu_6 \sin(\theta_2 + \theta_3) \left(\dot{\theta}_2 + \dot{\theta}_3 \right)$$
$$\times \left(2\dot{\theta}_1 + \dot{\theta}_2 + \dot{\theta}_3 \right)$$

$$C_2 = \mu_5 \sin \theta_2 \dot{\theta}_1^2$$
$$- \mu_5 \sin \theta_3 \left[\dot{\theta}_3 \left(2\dot{\theta}_1 + \dot{\theta}_2 + \dot{\theta}_3 \right) \right]$$
$$+ \mu_6 \sin(\theta_2 + \theta_3) \dot{\theta}_1^2$$

$$C_3 = \mu_5 \sin \theta_3 \left(\dot{\theta}_1 + \dot{\theta}_2 \right) + \mu_6 \sin \left(\dot{\theta}_2 + \dot{\theta}_3 \right) \dot{\theta}_1^2$$

The terms μ_1, μ_2, μ_3 are functions of the masses $(m_1, m_2, m_3) = (0.05, 0.04, 0.03) \, Kgr$ and the lengths $(l_1, l_2, l_3) = (0.0508, 0.0254, 0.01905) \, m$ of the 3 bones of the index finger. They are specified as $mu_1 = (m_1 + m_2 + m_3), \mu_1 = (m_1 + m_2 + m_3) l_1^2, \mu_3 = m_3 l_3^2, \mu_4 = (m_2 + m_3) l_1 l_2, \mu_5 = m_3 l_2 l_3$ and $\mu_6 = m_3 l_1 l_3$.

III. COMPLEXITY OF THE INDEX FINGER.

Based on the model of the index finger dynamics there is a significant amount of complexity which results from two facts:

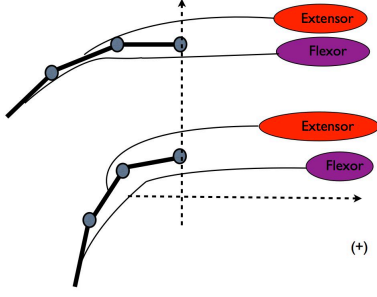1) Almost all tendons create rotations around the three joints of the index finger. This characteristic creates

Fig. 1. Length profile of active tendons for the 0.3 s tapping movement starting from the initial configuration $\theta_0 = (60^o, -90^o, -18^o)$ to target configuration $\theta^* = (-60^o, -45^o, -15^o)$.

a sophisticated actuation mechanism in which the role of each tendon is poorly understood. To further understand the complexity it suffices to consider the structure of the moment arm matrix:

$$\mathbf{M}_\Theta = \begin{bmatrix} * & * & * & * & * & * & * \\ * & * & 0 & * & * & * & * \\ * & 0 & 0 & * & * & * & * \end{bmatrix} \quad (34)$$

Clearly all tendons contribute to rotations around the 3 joins of the index finger. Exception is the FDS, which does not contribute to rotations around the MCP joint and the RI, that does not contribute to rotations around the MCP and PIP.

2) The constraints in controls reduce the space of possible control solutions. These constraints come from the fact that tendon only pull and they do not push. This property of tendons driven systems in combination with the structure of the moment arm matrix make the process of finding a control, challenging.

One of the main questions we ask in this paper is related to the role of each tendon. In general, there is no *a priori* expectation regarding the role of each tendon because, in multi-articular tendons, the resultant change in length depends on the combined changes at all joints. Nevertheless, one could come up with a hypothesis for tendons such as the FDS, FDP and EC, EI since their attachment on the bone structure of index finger is similar to the one of the flexor and extensor as they are illustrated in figure 1. Thus, for FDS and FDP we expect that their length increases while for the EC and EI their length should decrease for the tapping task. For the rest tendons RI,UI and LU there is no *a priori* expectation as to whether they act as extensors of flexors for the task of tapping

IV. ITERATIVE STOCHASTIC OPTIMAL CONTROL

We consider the nonlinear dynamical system described by the stochastic differential equation that follows:

$$\mathbf{dx} = f(\mathbf{x}, \mathbf{u})dt + F(\mathbf{x}, \mathbf{u})\mathbf{d}\omega$$

where $\mathbf{x} \in \Re^{n \times 1}$ is the state, $\mathbf{u} \in \Re^{m \times 1}$ is the control and $\omega \in \Re^{p \times 1}$ Brownian motion noise with variance $\sigma^2 I_{p \times p}$. The stochastic differential equation above corresponds to a rather general class of dynamical systems which are found in robotics and biomechanics. The term $h(\mathbf{x}(T))$ is the terminal cost in the cost function while the $\ell(\tau, \mathbf{x}(\tau), \pi(\tau, \mathbf{x}(\tau)))$ is the instantaneous cost rate which is a function of the state $\mathbf{x}$ and control policy $\pi(\tau, \mathbf{x}(\tau))$. The cost-to - go $v^\pi(\mathbf{x}, t)$ is defined as the expected cost accumulated over the time horizon $(t_0, ..., T)$ starting from the initial state $\mathbf{x}_t$ to the final state $\mathbf{x}(T)$.

$$v^\pi(\mathbf{x}, t) = E\left[h(\mathbf{x}(T)) + \int_{t_0}^T \ell(\tau, \mathbf{x}(\tau), \pi(\tau, \mathbf{x}(\tau))) d\tau \right]$$

The expectation above is taken over the noise ω. We next discretize the deterministic dynamics and therefore we will have $\bar{\mathbf{x}}_{t_{k+1}} = \bar{\mathbf{x}}_{t_k} + \Delta t f(\bar{\mathbf{x}}_{t_k}, \bar{\mathbf{u}}_{t_k})$. Furthermore the deterministic dynamics are linearized according to the equation that follows around $\bar{\mathbf{x}}_{t_k}$

$$\delta \mathbf{x}_{t_{k+1}} + \bar{\mathbf{x}}_{t_{k+1}} = \bar{\mathbf{x}}_{t_k} + \delta \bar{\mathbf{x}}_{t_k} \Delta t f(\bar{\mathbf{x}}_{t_k} + \delta \bar{\mathbf{x}}_{t_k}, \bar{\mathbf{u}}_{t_k} + \delta \bar{\mathbf{u}}_{t_k})$$

The first order approximation of the nonlinear dynamics leads the linearized dynamics: $\delta \mathbf{x}_{t_{k+1}} = A_k \mathbf{x}_{t_k} + B_k \delta \mathbf{u}_{t_k} + \Gamma_k (\delta \mathbf{u}_{t_k}) \xi_{t_k}$ where Γ_k is the noise transition matrix that is control depended and it is defined as follows:

$$\Gamma_k (\delta \mathbf{u}_{t_k}) = \begin{bmatrix} \mathbf{c}_{1,k} + C_{1,k} \delta \mathbf{u}_{t_k} & \cdots & \mathbf{c}_{p,k} + C_{p,k} \delta \mathbf{u}_{t_k} \end{bmatrix}$$

with $\mathbf{c}_{i,k} = \sqrt{dt} F^{(i)}$ and $C_{i,k} = \sqrt{dt} \partial F^{(i)} / \partial \delta \mathbf{u}$. The state and control transition matrices are expressed as: $A_k = I + dt \partial \mathbf{f} / \partial \mathbf{x}$ and $B_k = dt \partial \mathbf{f} / \partial \mathbf{u}$. The quadratic approximation of the cost function is given as follows:

$$Cost_k = q_k + \delta \mathbf{x}_{t_k}^T \mathbf{q} + \frac{1}{2} \delta \mathbf{x}_{t_k}^T Q_k \mathbf{x}_{t_k} \quad (35)$$
$$+ \delta \mathbf{u}_{t_k}^T \mathbf{r} + \frac{1}{2} \delta \mathbf{u}_{t_k}^T R_k \mathbf{u}_{t_k} + \delta \mathbf{x}_{t_k}^T P_k \mathbf{u}_{t_k}$$

where the terms : $q_k, \mathbf{q}_k \in \Re^{n \times 1}, Q_k \in \Re^{n \times n}, \mathbf{r}_k \in \Re^{m \times 1}, R_k \in \Re^{m \times m}, P_k \in \Re^{n \times m}$ are defined as: $q_k = dt \ \ell$, $\mathbf{q}_k = dt \ \partial \ell / \partial \mathbf{x}$, $Q_k = dt \ \partial^2 \ell / \partial \mathbf{x} \partial \delta \mathbf{x}$, $P_k = dt \ \partial^2 \ell / \partial \mathbf{u} \partial \mathbf{x}$, $\mathbf{r}_k = dt \ \partial \ell / \partial \delta \mathbf{u}$ and $R_k = dt \ \partial^2 \ell / \partial \mathbf{u} \partial \mathbf{u}$. In [3],[2] we have shown by induction that the cost to go $v_k (\delta \mathbf{x})$ is quadratic and therefore it has the form: $v_k (\delta \mathbf{x}) = s_k + \mathbf{s}_{k+1}^T \delta \mathbf{x} + \delta \mathbf{x}^T S_{k+1} \delta \mathbf{x},$

where the terms $s_k, \mathbf{s}_{k+1}$ and S_{k+1} are backward propagated from the terminal or goal state to the initial state. More precisely starting with the terminal conditions $s_{k+1} = q_T, \mathbf{s}_{k+1} = \mathbf{q}_T$ and $S_{k+1} = Q_T$, for $k = T - 1$ we find the following terms:

$$\mathbf{g} = \mathbf{r}_k + B_k^T s_{k+1} + \sum_i C_{i,k}^T S_{k+1} c_{i,k}$$

$$G = P_k + B_k^T S_{k+1} A_k \tag{36}$$

$$H = \sum_i C_{i,k}^T S_{k+1} C_{i,k} + B_k^T S_{k+1} B_k + R_k \mathbf{g}$$

By using the terms above the we can now calculate the correction in the control policy $\delta \mathbf{u}_{t_k}$ is formulated as $\delta \mathbf{u}_{t_k} = -H^{-1} \left(\mathbf{g} + G \delta \mathbf{x}_{t_k} \right)$ or in a more compact form $\delta \mathbf{u}_{t_k} = l_k + L_k \delta \mathbf{x}_{t_k}$ where $l_k = -H^{-1} \mathbf{g}$ and $L_k = -H^{-1} G$. As we can see the correction in the control policy consist of an open loop gain l_k and a close loop gain L_k which guarantees local stability around the point of linearization of the nonlinear dynamics. Since the open and close loop gains l_k and L_k have been specified the next step is the backward propagation of the terms $s_k, \mathbf{s}_{k+1}$ and S_{k+1}. This backward propagation is expressed by the equations that follow:

$$S_k = Q_k + A_k^T S_{k+1} A_k + L_k^T H L_k + L^k G + G^T L_k$$

$$\mathbf{s}_k = \mathbf{q}_k + A_k^T \mathbf{s}_{k+1} + L_k^T H l_k + G^T L_k + L_k^T \mathbf{g} \tag{37}$$

$$s_k = q_k + s_{k+1} + \frac{1}{2} \sum_i c_{i,k}^T S_{k+1} c_{i,k} + \frac{1}{2} l_k^T H l_k + l_k^T \mathbf{g}$$

The control policy at the next iteration is given by the adding the correction $\delta \mathbf{u}_{t,\dots,T}^{(i)}$ in the control policy of the current iteration. Therefore we will have that $\mathbf{u}_{t,\dots,T}^{(i+1)} = \mathbf{u}_{t,\dots,T}^{(i)} + \delta \mathbf{u}_{t,\dots,T}^{(i)}$. Using the updated control policy $\mathbf{u}_{t,\dots,T}^{(i+1)}$ and by propagating the nonlinear dynamics a new trajectory is generated in state space. The linear and quadratic approximation of the dynamics and cost are found and the algorithms is repeated again until convergence. The update law of the control policy above, changes if one considers constrains in control of the kind $\mathbf{u}_{min} \preceq \mathbf{u} \preceq \mathbf{u}_{max}$ where $\mathbf{x} \preceq \mathbf{y}$ is defined as the element-wise inequality between the two vectors $\mathbf{x}$ and $\mathbf{y}$. In this case, the update law of the current control policy is expressed by the equations:

$$\mathbf{u}_c = \max \left(\mathbf{u}_{\min}, \min \left(\mathbf{u}_{t_k}^{(i)} + \delta \mathbf{u}_{t_k}^{(i)}, \mathbf{u}_{\max} \right) \right)$$

$$\mathbf{u}_{t_k}^{(i+1)} = \mathbf{u}_c, \qquad \forall t < t_k < T$$

The control law $\delta \mathbf{u}_{t_k} = -H^{-1} \left(\mathbf{g} + G \delta \mathbf{x}_{t_k} \right)$ is the optimal one for as long as the matrix H is positive definite. As
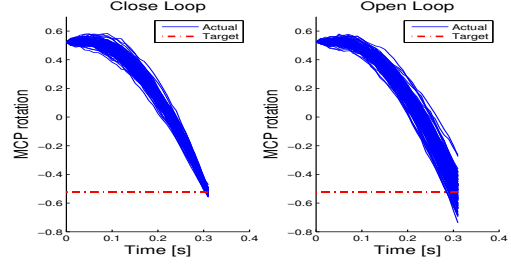

Fig. 2. The stochastic optimal feedback controller reduces the variability and perturbations MCP rotation.

we have shown in [3],[2] the cost-to-go function $v_\pi(\delta \mathbf{x})$ depends on the control law $\delta \mathbf{u}_k = \pi_k(\delta \mathbf{x})$ through the term $\alpha(\delta \mathbf{x}, \delta \mathbf{u}) = \delta \mathbf{u}^T(\mathbf{g} + G \delta \mathbf{x}) + \frac{1}{2} \delta \mathbf{u}^T H \delta \mathbf{u}$. Therefore minimization of the cost to go function is equivalent to the minimization of the quadratic function $\alpha(\delta \mathbf{x}, \delta \mathbf{u})$ which is convex iff the its Hessian $H > 0$. In highly dimensional dynamical systems H might loose its positive definiteness. In such cases we follow an approach similar to Levenberg-Marquardt : (1) compute the eigenvalue decomposition of H, $[V, D] = eig(H)$ (2) replace all the negative elements of the diagonal matrix with 0 (3) add a small positive number λ to the diagonal of D (4) set $H = VDV^T$ using the modified diagonal matrix D from the steps (2) and (3). The iLQG algorithm in a pseudocode form is illustrated in table (IV)

Finally, to see the effectiveness of the stochastic optimal feedback controller we illustrate in figure 2 the effect of noise in the kinematic trajectories of the MCP joint for the open loop and close loop case. In the open loop case only the open loop gain l_k is applied to the system. In the close loop case both open l_k and close loop gain L_k are applied. As we can see, under the presence of perturbation and noise in the dynamics the feedback gain reduces the variability of the trajectories towards the target. Similar behavior is observed for the kinematic trajectories of PIP and DIP joints.

V. RESULTS AND DISCUSSION

We apply the iLQG to the model of the index finger to generate a 400 ms tapping task. Note that for the tapping task we do not assume any desired trajectory(none desired by us, but algorithmically one will be converged upon as the iterative optimization proceeds), and the immediate cost function $\ell(\tau, \mathbf{x}(\tau), \pi(\tau, \mathbf{x}(\tau)))$ is only function of the controls and not function of the state. Therefore it is formulated as: $\ell(\tau, \mathbf{x}(\tau), \pi(\tau, \mathbf{x}(\tau))) = \pi^T R_k \pi$ with control cost weight matrix $R_k = r I_{7 \times 7}$ and $r = 0.0000001$. The terminal cost $h(\mathbf{x}(T))$ is specified as $h(\mathbf{x}(T)) = (\theta - \theta^*)^T Q (\theta - \theta^*)$ with $Q = 1000 I_{3 \times 3}$. The parameter $\theta^* = (-60^o, -45^o, -15^o)$
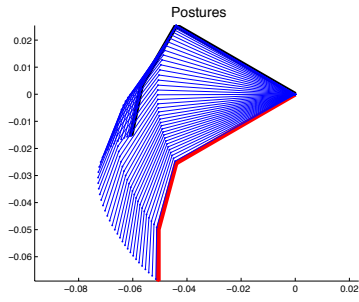
Fig. 3. Sequence of finger postures for the, 0.4s duration, tapping movement starting from the initial configuration $\theta_0 = (60^o, -90^o, -18^o)$ to target configuration $\theta^* = (-60^o, -45^o, -15^o)$.
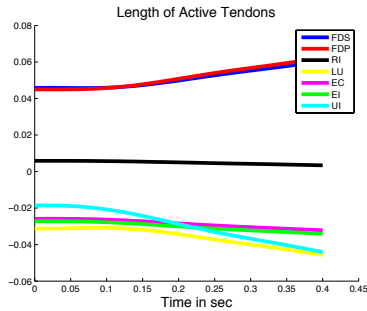

Fig. 5. Length profile of the passive tendons for the 0.4s tapping movement starting from the initial configuration $\theta_0 = (60^o, -90^o, -18^o)$ to target configuration $\theta^* = (-60^o, -45^o, -15^o)$.

Fig. 4. Length profile of active tendons for the 0.4s tapping movement starting from the initial configuration $\theta_0 = (60^o, -90^o, -18^o)$ to target configuration $\theta^* = (-60^o, -45^o, -15^o)$.

Fig. 6. Tendon tensions for 0.4s tapping movement starting from the initial configuration $\theta_0 = (60^o, -90^o, -18^o)$ to target configuration $\theta^* = (-60^o, -45^o, -15^o)$.

is the target configuration of the index finger just before contact occurs while the initial configuration is $\theta_0 = (60^o, -90^o, -18^o)$.

Figure (3) illustrates the sequence of postures during tapping, starting from the initial posture in black and reaching the target posture in red. In figure (4) the lengths of the active tendons are illustrated for the time horizon of 0.4 s during tapping. Clearly the lengths of the active tendons are specified by the geometry of the system as defined by the moment arm model. That is, when a joint rotates, all active tendons that cross it must change length appropriately. Note that by 'length we mean what is called the 'excursion biomechanics. That is, this is the amount by which the *musculotendon* as a whole needs to shorten or lengthen to keep the tendon from going slack, or from locking the joint rotation [6] 1. Typically, this change in the *musculotendon* is accommodated by shortening or lengthening of the muscle fibers given that the tendon is sufficiently stiff to only change its length by a small amount (like what we see in the passive tendons in our model). As we can see during this downward stroke of the tapping motion, the FDS, FDP tendons
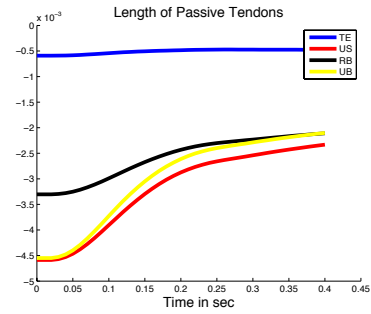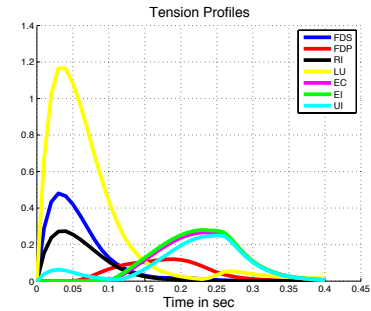
increase their length (i.e., we defined positive length changes when the proximal end of the tendon moves proximally, towards the elbow) while the main extensors of the index EC and ES decrease their length (i.e., we defined negative length changes as the proximal end of the tendon moving distally, towards the fingertip). This corresponds correctly to the intuition that the flexor *musculotendons* will shorten, while the extensor *musculotendons* will lengthen. The tendons UI and LU decrease their length and therefore behave as extensors, which can be explained by their insertions on the extensor mechanism. The RI remains at a constant length in this model because its line of action passes close to the center of rotation. RI is most often considered an abductor of the MCP joint, and at times a flexor of the MCP that our equations for moment arm do not emphasize without loss of generality. The changes in the length of UI and LU create rotations around all joins of the index finger while the length reduction of RI creates rotation in the MCP join.

Figure (5) illustrates the changes in length of the passive tendons TE, ES, RB and UB of the index finger. As we observe, the change in the length of the passive tendons is

of three orders of magnitude smaller than the corresponding length change of the active tendons. This observation is compatible with the passive nature of TE,ES, RB and UB and its role to pass the force applied by the active tendons to most distant ligament of the index finger.

Figure (6) illustrates the forces applied on the actuating tendons FDS, FDP, RI, LU, EC, EI, UI. According to figure (6) there are three overlapping phases. More precisely in the first phase, that is from 0 to 150ms, the applied forces on LU, FDS and RI reach their peak value while there is an increase in the force on FDP. In the second phase, that is from 100ms to 230ms, the force on FDP reaches its peak, the forces on LU, FDS and RI are decreasing and the forces on UI, EI and EC are increasing. Finally in the last phase, that is defined is the time interval from 0.15ms to 0.4ms, the forces on tendons UI, EI and EC reach their maximum value while the applied forces for the rest of the tendons are very small.

Our stochastic optimal controller gives us the complete time history of the tensions in the active tendons see figure (6). Knowledge of these tensions is of critical importance to the field of neuromuscular control of the hand. This information sheds light into the underlying patterns of force production at the level of individual muscles because these tensions are presumably provided by eccentric and concentric contractions of the muscles, which are in turn regulated by a neural command that interacts with active and passive properties of muscle [6]. At another level, the product of tendon tensions and *musculotendon* lengths and velocities reveals the work and power done by individual *musculotendons*. Note that because most muscles are active most of the time, there are invariably some muscles that do positive or negative work (i.e., they are sources and sinks of mechanical energy, respectively). Negative work is done by a muscle when its *musculotendon* is lengthening while its tendon has non-zero tension. The delicate interplay among *musculotendons* at the level of tensions, work, power and neural activation (command signal) during such dynamical tasks are now for the first time elucidated by these simulations. While we do not claim that these first simulations are necessarily physiologically valid (see future work), the importance of the fact that we are now for the first time able to describe at least some feasible solutions to the necessary and sufficient interplay of control signals needed to perform such a task cannot be overemphasized.

VI. CONCLUSIONS AND FUTURE WORK

In this work we present the application of stochastic optimal feedback control framework to a full tendon driven model of the index finger. Our simulations suggests that stochastic feedback control can successfully handle the highly nonlinear dynamics of the index finger which result from the addition of tendon model. Furthermore, the underlying biomechanics are better understood since the role of the extensors and flexors is investigated and the synergetic control strategy of the tendon tensions is analyzed. To our knowledge this paper is the first use of optimal control for the index finger with realistic complexity in the tendon paths.

One of the next steps for future research is to repeat the same study for different movements as well as different models of the moment arm matrix. The main goal is to investigate the sensitivity of the underlying control strategies with respect to different actuation characteristics and model variations of the index finger. Furthermore, extensions for the case of 3D movements will be also considered. In this case the dimensionality of the state vector will increase. On the biomechanics side, we can use the predicted tendon length and velocity profiles for comparison with experimental data. Unfortunately, noninvasive technology to measure tendon lengths in live human subjects is still under development and it faces many challenges. However we believe that in the near future we will be in the position to make such comparisons.

VII. ACKNOWLEDGMENTS

REFERENCES

[1] N Brook, Mizrahi J, Shoham M, and Dayan J. A biomechanical model of the index finger dynamics. *Medical Engineering Physics.*, 17:54–63, 1995.

[2] W Li and E. Todorov. Iterative linearization methods for approximately optimal control and estimation of non-linear stochastic systems. *International Journal of Control*, 80(12):1439–1453, 2007.

[3] E Todorov and W. Li. A generalized LQG method for locally optimal feedback control of constrained nonlinear stochastic systems. *In proceedings of the American Control Conference*, 2005.

[4] M Venkadesan and F.J. Valero-Cuevas. Effects of time delays on controlling contact transitions. *Royal Society*, 2008.

[5] M Venkadesan and F.J. Valero-Cuevas. Neural control of motion-to force transitions with the fingertip. *The journal of Neuroscience*, 28(6):1366–1373, 2008.

[6] F. E. Zajac. Muscle and tendon: properties, models, scaling, and application to biomechanics and motor control. *Crit. Rev. Biomed. Eng.*, 17(4):350 – 411, 1989.